frontiers | Frontiers in Materials

TYPE Mini Review
PUBLISHED 10 January 2024
DOI 10.3389/fmats.2023.1345592

OPEN ACCESS

EDITED BY
Emilia Morallon,
University of Alicante, Spain

REVIEWED BY
Lin Wei,
Lam Research, United States
Ramiro Ruiz Rosas,
University of Malaga, Spain

*CORRESPONDENCE
Zheng-Ze Pan,
zigzag.mpan@gmail.com,
pan.zhengze.e6@tohoku.ac.jp
Hirotomo Nishihara,
hirotomo.nishihara.b1@tohoku.ac.jp

RECEIVED 28 November 2023
ACCEPTED 19 December 2023
PUBLISHED 10 January 2024

CITATION
Pirabul K, Pan Z-Z and Nishihara H (2024), Structural control of nanoporous frameworks consisting of minimally stacked graphene walls.
Front. Mater. 10:1345592.
doi: 10.3389/fmats.2023.1345592

Structural control of nanoporous frameworks consisting of minimally stacked graphene walls

Kritin Pirabul[1], Zheng-Ze Pan[2]* and Hirotomo Nishihara[1,2]*

[1]Institute of Multidisciplinary Research for Advanced Materials, Tohoku University, Sendai, Miyagi, Japan, [2]Advanced Institute for Materials Research (WPI-AIMR), Tohoku University, Sendai, Miyagi, Japan

This mini-review provides an in-depth analysis of the formation and post-processing of nanoporous graphene materials *via* methane chemical vapor deposition (CH_4-CVD) using nanostructured metal oxide templates, including Al_2O_3, MgO, and SiO_2. Initially, the formation of graphene sheets is discussed in terms of the role of CH_4-CVD, the influence of templates, and the underlying mechanism for tailoring the structures of the graphene-based materials. Following this, the discussion extends to the post-graphene formation process. We focus on key steps, including template removal and graphene repair *via* zipping reactions at high temperatures. Additionally, we evaluate the conditions to prevent undesired structural transformations. The correlation between the structural features and transformations occurring during post-processing is also examined. The materials fabricated through these methods exhibit impressive properties of high porosity, minimal edge sites, superior oxidation resistance, and elasticity, positioning them as promising materials in various applications.

KEYWORDS

graphene-based materials, metal oxide templates, chemical vapor deposition, high temperature annealing, nanostructure engineering

1 Graphene-based nanoporous materials

Graphene, an allotrope of carbon, appears as a monolayer consisting of sp^2 hybridized carbon atoms arranged in a hexagonal lattice configuration. Due to its monolayer structure, it presents an extraordinarily high theoretical specific surface area of approximately 2,627 $m^2\ g^{-1}$ (Siqueira and Oliveira, 2017; Nishihara and Kyotani, 2018). The extensive π-conjugation that arises from orbital hybridization imparts extraordinary electron mobility (Morozov et al., 2008), remarkable thermal conductivity (Balandin et al., 2008), robust chemical stability (Jiang et al., 2007), and outstanding elasticity (Lee et al., 2008) to graphene materials. These fascinating attributes have captivated researchers across various fields, exploring its diverse potential applications, such as separators (Dasgupta et al., 2018; Park et al., 2018), material additives (Pantea et al., 2003; Casanova et al., 2020), catalyst supports (Yoshii et al., 2020), electrochemical devices (Lu et al., 2020; Atwa et al., 2021), and heat pumps (Nomura et al., 2019b). Despite its unique properties, the intrinsic two-dimensional (2D) nature of graphene sheets renders them prone to stacking interactions, altering their distinctive properties, particularly the reduction in exposed surface area and electron mobility (Liu et al., 2010; Fan et al., 2016; Ito et al., 2018;

Sun et al., 2020). Consequently, the presence of this stacking structure poses a formidable hurdle for graphene to attain its theoretical performance, especially in electrochemical devices. The constrained surface area impedes the full accessibility of active sites and the diffusion of ions and electrons, thereby undermining the performance in electrochemical applications. To overcome the issue, transforming 2D graphene layers into well-organized and interconnected nanoporous frameworks has emerged as an effective approach.

The concept of fabricating graphene into a nanoporous framework has been proposed as a strategy to prevent restacking and preserve the intrinsic characteristics of graphene. The development of porosity also enhances the mass transfer efficiency within the graphene framework (Tang et al., 2019a; Anil Kumar et al., 2023). Thus, nanoporous graphene-based materials are highly promising for a range of electrochemical applications, such as fuel cells (Ohma et al., 2021), supercapacitors (Nomura et al., 2019a), lithium-sulfur batteries (Lu et al., 2020), and lithium-oxygen batteries (Yu et al., 2023a; Yu et al., 2023b; Shen et al., 2023). Considering the importance of distinctive properties for different applications, it becomes crucial to accurately optimize both the porosity and surface chemistry of graphene. This optimization is essential in order to maximize performance in specific applications. Regarding this, the traditional activation procedure falls short of delivering precise control of nanostructures. More advanced methods, such as template-assisted GO assembly (Huang et al., 2012; Zhang et al., 2014; Rodríguez-Mata et al., 2019) and template carbonization of impregnated organic substrates (Fan et al., 2012; Peng et al., 2014), offer better structural controllability. However, both approaches face challenges in achieving exact control over the graphene formation process. They often result in graphene materials that display characteristics such as stacked arrangements, heteroatomic defects, or amorphous graphene walls (Vix-Guterl et al., 2002; Ham et al., 2014; Nishihara and Kyotani, 2018). The first nanoporous material composed of single-layer graphene frameworks is zeolite-templated carbons (ZTCs) synthesized by a hard template method in 2000 (Ma et al., 2000; Nishihara et al., 2009; 2018). Although ZTCs possess an extremely high specific surface area of up to 4,000 $m^2\ g^{-1}$ and ordered micropores with a uniform pore size of 1.2 nm, their frameworks are defective and have a great number of edge sites, making them chemically and electrochemically not highly durable (Nishihara and Kyotani, 2018). On the other hand, the chemical vapor deposition (CVD) process on inorganic substrates or nanoparticles has been unequivocally proven as the most feasible way for the large-scale production of graphene-based materials possessing a high crystallinity and large specific surface area (Shi et al., 2015; Shu et al., 2015; Lin et al., 2018).

2 Graphene formation via the CVD process

CVD is a highly efficient technique to deposit graphene layers onto solid surfaces through the heterogeneous decomposition of carbon precursor gas. Using three-dimensional (3D) substrates as templates of CVD allows the fabrication of composites comprising templates coated with defective graphene. These composites can be subsequently subjected to template removal processes to obtain nanoporous graphene-based material. The CVD approach typically involves four elementary steps: i) introduction of a gaseous precursor into the template surface; ii) decomposition of the precursor to form active carbon species; iii) formation of graphene nuclei from the active carbon species; iv) epitaxial growth and coalescence of the graphene nuclei (Lin et al., 2018; Sun et al., 2020). It is vital to understand and eventually control these stepwise reactions to tailor the final product to meet the design specifications (Lin et al., 2018). To date, extensive studies have been conducted to unravel the intricate relation between the distinctive characteristics of the product and the influential factors that govern the graphene growth mechanism during CVD. In particular, aspects such as the role of hydrogen (Vlassiouk et al., 2011), the rate-limiting step (Bhaviripudi et al., 2010), the decomposition of various precursor gases (Chen et al., 2017), operating temperature and/or pressure (Hwang et al., 2013). Moreover, the integration of *in situ* analyses [such as Raman spectroscopy (Al-Hazmi et al., 2016; Tsakonas et al., 2021) and spectroscopic ellipsometry (Losurdo et al., 2011)], combined with theoretical calculations, has been recently adopted to acquire explicit insights into the underlying reaction kinetics during CVD growth (Wang et al., 2022). Most studies consistently converge on a similar conclusion, emphasizing the catalytic ability of the template for the initial decomposition reactions of the precursor gas as a pivotal factor determining the growth mechanism and quality of the resultant graphene. For instance, the lack of catalytic activity in templates or the utilization of unsaturated hydrocarbons with low dissociation energies in CVD often leads to defective graphene and amorphous carbon formation due to competing or dominating homogeneous gas-phase reactions (Abdullah et al., 2017; Lin et al., 2018; Chen et al., 2019). Notably, metallic templates such as Cu and Ni have demonstrated remarkable catalytic ability in promoting graphene growth with excellent crystallinity through the dissociation of thermally stable precursor gas of CH_4 (Reina et al., 2009; Li et al., 2011). However, the growth mechanisms of graphene on Ni typically lead to the formation of nonuniform multilayer graphene. This is because the dissociated carbon can continuously dissolve into the bulk of Ni due to its high solubility at CVD operating temperatures. Subsequently, the carbon solubility in Ni decreases at a lower temperature during the cooling step, supersaturating the carbon concentration and participating in the undesired graphene formation (Figure 1A) (Edwards and Coleman, 2013). On the other hand, this graphene segregation does not occur on Cu due to its low solubility for carbon. In addition, the graphene growth on Cu surface is found to be kinetically fast while self-limiting in forming bi- and multilayer configurations. This endows the Cu surface with superior controllability and uniformity towards the monolayer graphene (Figure 1B) (Li et al., 2009). Nevertheless, the fabrication of nanoporous graphene-based materials with regulated nanoporosity *via* CVD requires the usage of 3D substrates with sufficient thermal stability, which poses intrinsic challenges for metal species as they are easily sintered at the reaction temperatures of CVD (Ito et al., 2014; Zhang et al., 2015; DeArmond et al., 2020). In this regard, the use of metal oxides such as MgO (Sunahiro et al., 2021), Al_2O_3 (Nishihara et al., 2016), and SiO_2 (Pirabul et al., 2023), which exhibit high thermal resilience,

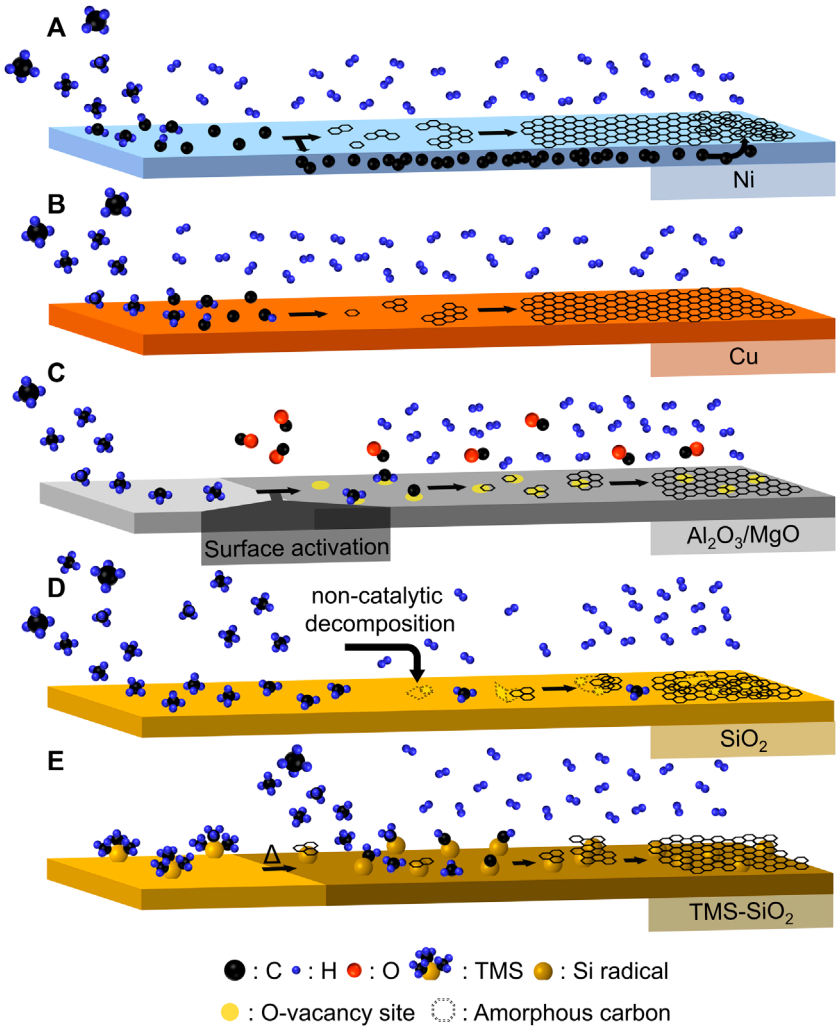

FIGURE 1
Schematic illustrations for the reaction mechanisms of CH_4-CVD on **(A)** Ni, **(B)** Cu, **(C)** Al_2O_3 or MgO, **(D)** SiO_2, and **(E)** TMS-SiO_2 surfaces.

is of interest for controlling the nanoporosity (<20 nm) of the resulting materials.

Applying 3D metal oxides as templates for CVD has several advantages, such as precise pore structure control, low cost, and being free from metal contamination in isolated graphene frameworks. However, a comprehensive understanding of the underlying mechanisms in graphene formation on these templates had not been clearly established, due to the inherent complexity (Lin et al., 2018). This hindered the optimization of the CVD process to realize the graphene sheets with high crystallinity and uniformity. Indeed, it has been widely recognized that the crucial steps dictating the graphene growth on non-metallic surfaces are tangling between thermal cracking of precursor gases, interactions between templates and carbon sources, and formation of nucleation sites (Sun et al., 2020). Recently, notable progress on the limiting step in transition metal-free CVD reactions at moderate temperatures below 1,000°C has been reported through the systematic study of comprehensive *in situ* CVD-thermogravimetric analysis (CVD-TG), CVD-gas chromatography (CVD-GC), and DFT calculations (Sunahiro et al., 2021).

Interestingly, Al_2O_3 and MgO, while having different catalytic properties as a solid acid and base, respectively, share a similar reaction mechanism. The surface of these templates is initially activated by the reaction between surface oxygen with CH_4, producing CO. This results in the creation of oxygen-vacancy sites that catalyze CH_4 dissociation and facilitate graphene nucleation (Figure 1C) with significantly lower apparent activation energies (*ca.* 130 kJ mol^{-1}) than on the carbon surface (205–236 kJ mol^{-1}) (Sunahiro et al., 2021). Additionally, the reaction rate for the first graphene layer is approximately three times faster than that for subsequent layers, enabling a preferential coating of the Al_2O_3 or MgO surface with predominantly single-layer graphene walls. SiO_2 is another intriguing template, owing to its diverse morphology and controllable nanostructure. However, its siloxane-based surface exhibits high inertness towards CH_4 dissociations (Figure 1D) (Chen et al., 2019). Therefore, carbon deposition had been possible

only *via* non-catalytic thermal decomposition of CH_4 on SiO_2, leading to the formation of graphene sheets with relatively lower quality (Chen et al., 2019). Various approaches have been devised to overcome the problem, including the manipulation of CVD conditions (Su et al., 2011; Kim et al., 2013) and the implementation of surface silylation modifications (Hoshikawa et al., 2014). Among those techniques, trimethylsilyl (TMS) surface modification has attracted considerable interests, given its promising applicability in industrialization. During the heating step, TMS groups encountered thermal decomposition, leading to the formation of polycyclic aromatic compounds and Si radicals (Figure 1E) (Pirabul et al., 2023). These Si radicals subsequently function as reactive center sites that initiate graphene growth with an apparent activation energy of 130 kJ mol^{-1}. This observed value is significantly lower than the value of 360 kJ mol^{-1} examined on the siloxane-based surfaces, comparable to the activation energies associated with the CH_4 decomposition without a catalyst (370–433 kJ mol^{-1}). The shift from the non-catalytic decomposition of CH_4 using a pristine SiO_2 template to the catalytic decomposition of CH_4 on the surface of TMS-SiO_2 brings favorable reaction kinetics. Using a thermodynamically stable carbon precursor gas such as CH_4 lowers the likelihood of undesired side reactions, thereby facilitating the formation of graphene structures that are less defective and more crystalline. The resulting graphene-coated SiO_2 composite from CH_4-CVD exhibits an electrical conductivity approximately 650 times higher than that of the counterpart material obtained through C_2H_2-CVD (Pirabul et al., 2023). These characteristics have allowed a unique role of the composite in biosensor applications (Fujii et al., 2023).

3 Post-graphene formation process

The controlled CVD process applied to nanostructured metal oxides forms the graphene frameworks with designed porosity. The subsequent template removal allows the isolation of the templated carbons (TCs). Further, high-temperature (HT) annealing (>1,000°C) is effective in removing edge sites *via* graphene-zipping reactions (Xia et al., 2023). However, undesired structural transformations can often occur during these processes depending on the properties of the TCs (Bi et al., 2015; Shi et al., 2015; Kamiyama et al., 2020). Hence, a comprehensive understanding of the interplays between carbon features and structural changes becomes essential to realize nanoporous graphene materials with precisely designed structures. The conventional method for removing metal oxides involves a wet-chemical process where the template is dissolved using acid or base solutions. However, the nanoporous framework consisting of single- or few-layer graphene sheets presents inherent flexibility (Nishihara et al., 2018), rendering it susceptible to structural contraction during the subsequent drying step due to the influence of capillary force. Consequently, additional localized contacts between the graphene walls are formed, reducing the specific surface area of obtained TCs (Figure 2A). It should be noted that the mobility of graphene sheets within a well-interconnected nanoporous framework is limited, thereby the capillary shrinkage-driven stacking is not expected to be a firm/seamless arrangement but rather denoted as loose stacking (Figure 2A) (Pirabul et al., 2023). In contrast, multi-layered graphene configurations that form during the bottom-up CVD process are relatively well-arranged and can be denoted as tight stacking (Figure 2A). A novel method for quantifying the formation of loosely stacked structures has been established, employing high-sensitivity vacuum temperature-programmed desorption (TPD) (Ishii et al., 2014). This sensible measurement allows the precise extraction of the specific surface area of the basal plane (S_{basal}) from the total specific surface area determined by the N_2 adsorption technique. S_{basal} is closely related to the arrangement of graphene layers, providing the evaluation of an average number of total stacking layers (N_{total}) and loose stacking layers (N_{loose}), according to the following Eqs 1, 2 (Pirabul et al., 2023).

$$N_{total} = S_{graphene}/S_{basal} \tag{1}$$

$$N_{loose} = N_{total} - N_{tight} \tag{2}$$

Here, $S_{graphene}$ is the geometrical specific surface area of single-layer graphene (2,627 $m^2\ g^{-1}$), and N_{tight} is the average number of tight stacking layers determined using the amount of deposited carbon onto the unit weight of templates ($w_{c\_gravimetric}$ [g g^{-1}]), as shown in Eq. 3 (Pirabul et al., 2023).

$$N_{tight} = \frac{w_{c\_gravimetric}}{S_{BET(template)} \times W_{graphene}} \tag{3}$$

$S_{BET(template)}$ and $W_{graphene}$ are the specific surface area of a parental template [$m^2\ g^{-1}$] and the areal weight of a single graphene layer (7.164×10^{-4} g m^{-2}), respectively.

It was revealed that the prevalence of loose stacking becomes more pronounced with the enlargement of pore size inherited from its parental template size (referring to the average diameter for spherical templates and the thickness for the plate template), as shown in Figure 2B (Pirabul et al., 2023). This observation can be described as the poor mechanical strength of large pores made of single-layer graphene. Furthermore, the morphology of the pores inherited from a template also impacts the degree of shrinkage. Specifically, slit-shaped pores show a higher tendency for contraction than spherical-shaped pores. A higher prevalence of loosely stacked structures is associated with increased contraction. This can lead to deviations from the intended porosity. Capillary shrinkage can be effectively suppressed by achieving tight stacking during the CVD process. This structure can improve the mechanical strength of the resulting nanoporous graphene. Hence, optimizing the CVD conditions to control the average number of tightly stacked graphene layers is a pivotal strategy to retain the replicated porosity upon the subsequent removal of the template. Additionally, the shrinkage can be alleviated by replacing residual water from chemical etching with a solvent that has lower surface tension, such as acetone, to mitigate capillary forces during drying. This strategy enhances the production of TCs with varied structures, boasting mean pore sizes between 5 and 70 nm (Nishihara et al., 2016; Sunahiro et al., 2021; Pirabul et al., 2023). These mesoporous graphene materials have an expansive specific surface area, reaching up to 2,277 $m^2\ g^{-1}$, nearing the geometrical surface areas of single-layer graphene (Nishihara et al., 2016; Sunahiro et al., 2021; Pirabul et al., 2023).

TCs, synthesized *via* CVD, normally demonstrate a distinctive evolution of gases (H_2, H_2O, CO, and CO_2) under high-temperature conditions, attributing to the H-terminated edge sites and oxygen

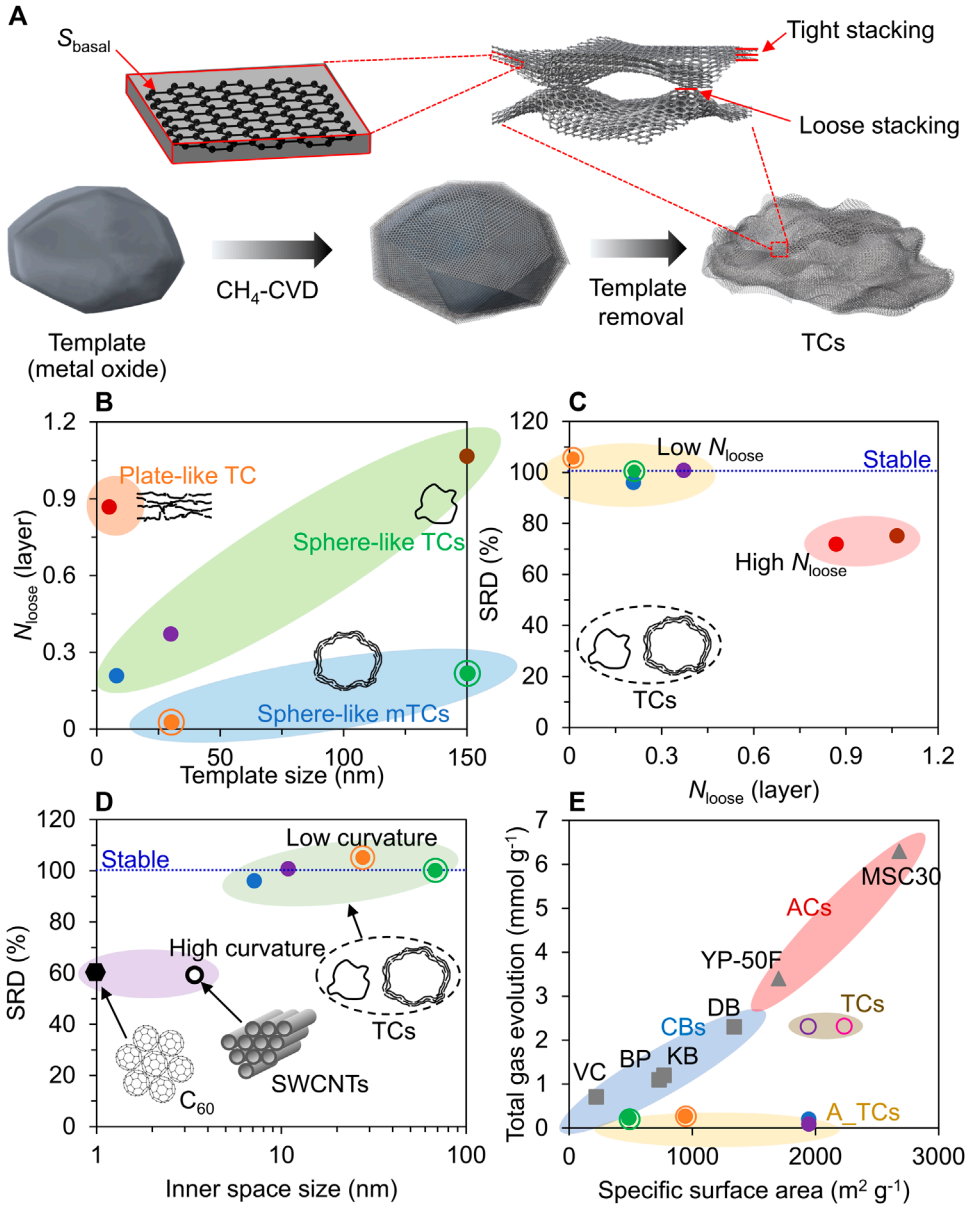

FIGURE 2
(A) Illustration for the synthesis procedure of TCs. **(B)** Correlation between N_{loose} of TCs with respect to its parental template size (referring to the average diameter for spherical templates and the thickness for the plate template). mTC refers to the TCs with an average number of tight stacking higher than 1.0. **(C, D)** The relationship of the SRD with **(C)** N_{loose} and **(D)** the inner space size. **(E)** Total gas evolution against the specific surface area for A_TCs, CBs (VC, BP, KB, and DB), and ACs (YP-50F; and MSC30). The CBs include VC (VULCAN XC72) from Cabot Co., DB (Denka acetylene black) from Denka Co., Ltd., KB (Ketjenblack EC300J) from Lion Specialty Chemicals Co., Ltd., and BP (BLACK PEARLS 2000) from Cabot Co. The ACs include YP-50F from Kuraray Chemical Co., Ltd. and MSC30 from Kansai Coke and Chemicals Co., Ltd. Reproduced from Pirabul et al. (2023), Copyright (2023), with permission from The Chemical Society of Japan. The data of TCs shown in **(E)** was taken from Sunahiro et al. (2021).

functional groups (Ishii et al., 2014). To date, TCs are often subjected to HT annealing to eliminate heteroatomic defects and merge graphene boundaries concurrently (Banhart et al., 2011; Yang et al., 2018). This refinement bestows the annealed TCs with improved durability and electron mobility, which are valuable for chemical or electrochemical applications. However, the structure of the graphene framework may be distorted at high temperatures, adversely affecting the porosity and overall performance. Recently, we introduced a new parameter, the structural retention degree (SRD), which is a quantitative measure for structural change during HT annealing at 1800°C. This parameter is defined by Eq. 4 (Pirabul et al., 2023).

$$\mathrm{SRD}\,[\%] = S_{\mathrm{basal(HT\_annealed)}} \times 100 / S_{\mathrm{basal}} \tag{4}$$

Here, $S_{basal(HT\_annealed)}$ and S_{basal} are the basal plane specific surface areas of the annealed TC and the pristine TC, respectively. It is found that loosely stacked graphene configurations are responsible for the structural alterations upon HT annealing (Figure 2C) (Pirabul et al., 2023). This phenomenon leads to the elongation of the stacked carbonaceous structures, consequently leading to a decrease in the specific surface area associated with the basal plane. The extension of the stacking configuration aligns well with the crystallographic changes observed through X-ray diffraction and Raman spectroscopy measurements (Pirabul et al., 2023). Furthermore, the high curvature surface of graphene sheets, characterized by small inner space sizes (referring to the inter π-electron cloud diameter for C_{60} and the pore sizes for SWCNTs and TCs), represents another structure vulnerable to thermally induced alternations. In essence, this surface tends to accumulate diminished strain energy, leading to the breaking of C-C bonds and prompting structural transformations upon HT annealing. Recent research has revealed that the critical threshold for inner space sizes, particularly in the 4–7 nm range, correlates with compromised thermal stability (Figure 2D) (Pirabul et al., 2023).

4 Resultant graphene materials

The aforementioned review underscores significant advancements in understanding the mechanisms behind graphene formation *via* CH_4-CVD using metal oxides (Al_2O_3, MgO, and SiO_2) as templates. It also sheds light on the structural transformations that take place during the post-graphene formation. These findings offer critical insights into the engineering of nanoporous graphene-based materials, especially focusing on the control of their porosity and surface chemical properties. Controlling carbon edge sites, which are recognized as initiators of corrosion reactions, is crucial for electrochemical device applications (Tang et al., 2019b). Concurrently, it is essential to optimize the porosity of nanoporous graphene materials. A valuable approach to quantifying the carbon edge sites in these carbon materials involves analyzing the comprehensive gas emission, including H_2, H_2O, CO, and CO_2, at 1800°C. This analysis can be conducted using a high-sensitivity vacuum TPD technique, offering insights into the microstructural properties of the templated carbons (Ishii et al., 2014). Conventional nanoporous carbons, including activated carbons (ACs) and carbon blacks (CBs), show a positive correlation between specific surface area and the number of carbon edge sites, as illustrated in Figure 2E. For instance, YP-50F, a commonly used AC in commercial electric double-layer capacitors, possesses a large specific surface area of 1,700 $m^2\ g^{-1}$ with a massive total gas evolution of 3.4 mmol g^{-1}. Thus, it has been challenging to achieve a high specific surface area and a minimal number of carbon edge sites (a small amount of total gas emission in TPD). By sharp contrast, the TCs subjected to post-annealing treatment at 1,800°C (denoted A_TCs) exhibit a negligible amount of edge sites (with gas evolution ranging from 0.09 to 0.27 μmol g^{-1}) along with a satisfied specific surface area (up to 1,946 $m^2\ g^{-1}$) and varying pore sizes inherited from their parent templates (Figure 2E). As a result, A_TCs reveal a higher oxidation resistance than YP-50F despite variations in their porosity characteristics (Pirabul et al., 2023). The concomitant realization of developed porosity and superior durability enables A_TCs to serve in various electrochemical devices, such as fuel cells, supercapacitors, and rechargeable batteries.

5 Conclusion and future perspective

The mechanisms driving the graphene formation process via CH_4-CVD on various 3D non-metallic templates have been illustrated in this mini-review. The achievement signifies a notable advancement in crafting uniformly coated 3D templates that consist of graphene sheets with high crystallinity. These composites are versatile platforms that can be applied effortlessly or further extracted into high-quality nanoporous graphene materials. The correlation between structural features and their transformations during template removal and HT annealing processes has also been revealed. These have paved the way for developing novel methodologies to prepare nanoporous graphene materials with minimally stacked graphene walls, designed mesoporosity, excellent crystallinity, and high oxidation resistance. The unique characteristics exhibited by these materials render them up-and-coming materials in a wide range of applications such as material additives, catalyst supports, and electrochemical devices. Furthermore, the insights gained from these studies provide a solid foundation for further explorations. For instance, a promising opportunity exists to delve into the unique characteristics exhibited by the recently classified structure referred to as loose stacking. Additionally, there is a prospect to enhance the accessibility of hierarchical structures within the graphene framework. Such explorations could lead to the discovery of even more versatile and advanced graphene-based materials with tailored properties for specific applications.

Author contributions

KP: Writing–original draft, Writing–review and editing. Z-ZP: Project administration, Supervision, Writing–review and editing. HN: Funding acquisition, Project administration, Supervision, Writing–review and editing.

Funding

The author(s) declare financial support was received for the research, authorship, and/or publication of this article. This work was supported by JSPS KAKENHI Grant no. 23H00227; JST SICORP Grant no. JPMJSC2112; JST A-STEP Grant no. JPMJTR22T6.

Conflict of interest

The authors declare that the research was conducted in the absence of any commercial or financial relationships that could be construed as a potential conflict of interest.

Publisher's note

References

Abdullah, H., Ramli, I., Ismail, I., and Yusof, N. (2017). Hydrocarbon sources for the carbon nanotubes production by chemical vapour deposition: a review. *Pertanika J. Sci. Technol.* 25, 379–396.

Al-Hazmi, F. S., Beall, G. W., Al-Ghamdi, A. A., Alshahrie, A., Shokr, F. S., and Mahmoud, W. E. (2016). Raman and ellipsometry spectroscopic analysis of graphene films grown directly on Si substrate via CVD technique for estimating the graphene atomic planes number. *J. Mol. Struct.* 1118, 275–278. doi:10.1016/j.molstruc.2016.04.028

Anil Kumar, Y., Koyyada, G., Ramachandran, T., Kim, J. H., Sajid, S., Moniruzzaman, M., et al. (2023). Carbon materials as a conductive skeleton for supercapacitor electrode applications: a review. *Nanomaterials* 13, 1049. doi:10.3390/nano13061049

Atwa, M., Li, X., Wang, Z., Dull, S., Xu, S., Tong, X., et al. (2021). Scalable nanoporous carbon films allow line-of-sight 3D atomic layer deposition of Pt: towards a new generation catalyst layer for PEM fuel cells. *Mater Horiz.* 8, 2451–2462. doi:10.1039/D1MH00268F

Balandin, A., Ghosh, S., Bao, W., Calizo, I., Teweldebrhan, D., Miao, F., et al. (2008). Superior thermal conductivity of single-layer graphene. *Nano Lett.* 8, 902–907. doi:10.1021/nl0731872

Banhart, F., Kotakoski, J., and Krasheninnikov, A. V. (2011). Structural defects in graphene. *ACS Nano* 5, 26–41. doi:10.1021/nn102598m

Bhaviripudi, S., Jia, X., Dresselhaus, M. S., and Kong, J. (2010). Role of kinetic factors in chemical vapor deposition synthesis of uniform large area graphene using copper catalyst. *Nano Lett.* 10, 4128–4133. doi:10.1021/nl102355e

Bi, H., Chen, I.-W., Lin, T., and Huang, F. (2015). A new tubular graphene form of a tetrahedrally connected cellular structure. *Adv. Mater.* 27, 5943–5949. doi:10.1002/adma.201502682

Casanova, A., Gomis-Berenguer, A., Canizares, A., Simon, P., Calzada, D., and Ania, C. O. (2020). Carbon black as conductive additive and structural director of porous carbon gels. *Materials* 13, 217. doi:10.3390/ma13010217

Chen, X.-D., Chen, Z., Jiang, W.-S., Zhang, C., Sun, J., Wang, H., et al. (2017). Fast growth and broad applications of 25-inch uniform graphene glass. *Adv. Mater.* 29, 1603428. doi:10.1002/adma.201603428

Chen, Z., Qi, Y., Chen, X., Zhang, Y. F., and Liu, Z. (2019). Direct CVD growth of graphene on traditional glass: methods and mechanisms. *Adv. Mat.* 31, e18. doi:10.1002/adma.201803639

Dasgupta, A., Matos, J., Muramatsu, H., Ono, Y., Gonzalez, V., Liu, H., et al. (2018). Nanostructured carbon materials for enhanced nitrobenzene adsorption: physical vs. chemical surface properties. *Carbon N. Y.* 139, 833–844. doi:10.1016/J.CARBON.2018.07.045

DeArmond, D., Zhang, L., Malik, R., Vamsi Krishna Reddy, K., Alvarez, N. T., Haase, M. R., et al. (2020). Scalable CVD synthesis of three-dimensional graphene from cast catalyst. *Mat. Sci. Eng. B* 254, 114510. doi:10.1016/j.mseb.2020.114510

Edwards, R. S., and Coleman, K. S. (2013). Graphene film growth on polycrystalline metals. *Acc. Chem. Res.* 46, 23–30. doi:10.1021/ar3001266

Fan, M., Feng, Z.-Q., Zhu, C., Chen, X., Chen, C., Yang, J., et al. (2016). Recent progress in 2D or 3D N-doped graphene synthesis and the characterizations, properties, and modulations of N species. *J. Mater Sci.* 51, 10323–10349. doi:10.1007/s10853-016-0250-8

Fan, Z., Liu, Y., Yan, J., Ning, G., Wang, Q., Wei, T., et al. (2012). Template-directed synthesis of pillared-porous carbon nanosheet architectures: high-performance electrode materials for supercapacitors. *Adv. Energy Mat.* 2, 419–424. doi:10.1002/aenm.201100654

Fujii, S., Yoshida, A., Chuong, T. T., Minegishi, Y., Pirabul, K., Pan, Z.-Z., et al. (2023). Development of microdrip enzyme device using carbon-coated porous silica spheres. *ACS Appl. Eng. Mater.* 1, 1426–1435. doi:10.1021/acsaenm.3c00103

Ham, H., Van Khai, T., Park, N.-H., So, D. S., Lee, J.-W., Gil Na, H., et al. (2014). Freeze-drying-induced changes in the properties of graphene oxides. *Nanotechnology* 25, 235601. doi:10.1088/0957-4484/25/23/235601

Hoshikawa, Y., Castro-Muñiz, A., Komiyama, H., Ishii, T., Yokoyama, T., Nanbu, H., et al. (2014). Remarkable enhancement of pyrolytic carbon deposition on ordered mesoporous silicas by their trimethylsilylation. *Carbon N. Y.* 67, 156–167. doi:10.1016/j.carbon.2013.09.075

Huang, X., Qian, K., Yang, J., Zhang, J., Li, L., Yu, C., et al. (2012). Functional nanoporous graphene foams with controlled pore sizes. *Adv. Mat.* 24, 4419–4423. doi:10.1002/adma.201201680

Hwang, J., Kim, M., Campbell, D., Alsalman, H. A., Kwak, J. Y., Shivaraman, S., et al. (2013). van der Waals epitaxial growth of graphene on sapphire by chemical vapor deposition without a metal catalyst. *ACS Nano* 7, 385–395. doi:10.1021/nn305486x

Ishii, T., Kashihara, S., Hoshikawa, Y., Ozaki, J., Kannari, N., Takai, K., et al. (2014). A quantitative analysis of carbon edge sites and an estimation of graphene sheet size in high-temperature treated, non-porous carbons. *Carbon N. Y.* 80, 135–145. doi:10.1016/j.carbon.2014.08.048

Ito, Y., Tanabe, Y., Qiu, H.-J., Sugawara, K., Heguri, S., Tu, N. H., et al. (2014). High-quality three-dimensional nanoporous graphene. *Angew. Chem. Int. Ed. Engl.* 53, 4822–4826. doi:10.1002/anie.201402662

Ito, Y., Tanabe, Y., Sugawara, K., Koshino, M., Takahashi, T., Tanigaki, K., et al. (2018). Three-dimensional porous graphene networks expand graphene-based electronic device applications. *Phys. Chem. Chem. Phys.* 20, 6024–6033. doi:10.1039/C7CP07667C

Jiang, D., Sumpter, B. G., and Dai, S. (2007). Unique chemical reactivity of a graphene nanoribbon's zigzag edge. *J. Chem. Phys.* 126, 134701. doi:10.1063/1.2715558

Kamiyama, A., Kubota, K., Nakano, T., Fujimura, S., Shiraishi, S., Tsukada, H., et al. (2020). High-capacity hard carbon synthesized from macroporous phenolic resin for sodium-ion and potassium-ion battery. *ACS Appl. Energy Mater.* 3, 135–140. doi:10.1021/acsaem.9b01972

Kim, H., Song, I., Park, C., Son, M., Hong, M., Kim, Y., et al. (2013). Copper-vapor-assisted chemical vapor deposition for high-quality and metal-free single-layer graphene on amorphous SiO2 substrate. *ACS Nano* 7, 6575–6582. doi:10.1021/nn402847w

Lee, C., Wei, X., Kysar, J. W., and Hone, J. (2008). Measurement of the elastic properties and intrinsic strength of monolayer graphene. *Science* 321, 385–388. doi:10.1126/science.1157996

Li, X., Cai, W., Colombo, L., and Ruoff, R. S. (2009). Evolution of graphene growth on Ni and Cu by carbon isotope labeling. *Nano Lett.* 9, 4268–4272. doi:10.1021/nl902515k

Li, X., Magnuson, C. W., Venugopal, A., Tromp, R. M., Hannon, J. B., Vogel, E. M., et al. (2011). Large-area graphene single crystals grown by low-pressure chemical vapor deposition of methane on copper. *J. Am. Chem. Soc.* 133, 2816–2819. doi:10.1021/ja109793s

Lin, L., Deng, B., Sun, J., Peng, H., and Liu, Z. (2018). Bridging the gap between reality and ideal in chemical vapor deposition growth of graphene. *Chem. Rev.* 118, 9281–9343. doi:10.1021/acs.chemrev.8b00325

Liu, C., Yu, Z., Neff, D., Zhamu, A., and Jang, Z. B. (2010). Graphene-based supercapacitor with an ultrahigh energy density. *Nano Lett.* 10, 4863–4868. doi:10.1021/nl102661q

Losurdo, M., Giangregorio, M. M., Capezzuto, P., and Bruno, G. (2011). Ellipsometry as a real-time optical tool for monitoring and understanding graphene growth on metals. *J. Phys. Chem. C* 115, 21804–21812. doi:10.1021/jp2068914

Lu, L., Pei, F., Abeln, T., and Pei, Y. (2020). Tailoring three-dimensional interconnected nanoporous graphene micro/nano-foams for lithium-sulfur batteries. *Carbon N. Y.* 157, 437–447. doi:10.1016/j.carbon.2019.10.072

Ma, Z., Kyotani, T., and Tomita, A. (2000). Preparation of a high surface area microporous carbon having the structural regularity of Y zeolite. *Chem. Commun.*, 2365–2366. doi:10.1039/B006295M

Morozov, S. V., Novoselov, K. S., Katsnelson, M. I., Schedin, F., Elias, D. C., Jaszczak, J. A., et al. (2008). Giant intrinsic carrier mobilities in graphene and its bilayer. *Phys. Rev. Lett.* 100, 016602. doi:10.1103/PhysRevLett.100.016602

Nishihara, H., Fujimoto, H., Itoi, H., Nomura, K., Tanaka, H., Miyahara, M. T., et al. (2018). Graphene-based ordered framework with a diverse range of carbon polygons formed in zeolite nanochannels. *Carbon N. Y.* 129, 854–862. doi:10.1016/j.carbon.2017.12.055

Nishihara, H., and Kyotani, T. (2018). Zeolite-templated carbons – three-dimensional microporous graphene frameworks. *Chem. Commun.* 54, 5648–5673. doi:10.1039/C8CC01932K

Nishihara, H., Simura, T., Kobayashi, S., Nomura, K., Berenguer, R., Ito, M., et al. (2016). Oxidation-resistant and elastic mesoporous carbon with single-layer graphene walls. *Adv. Funct. Mat.* 26, 6418–6427. doi:10.1002/adfm.201602459

Nishihara, H., Yang, Q.-H., Hou, P.-X., Unno, M., Yamauchi, S., Saito, R., et al. (2009). A possible buckybowl-like structure of zeolite templated carbon. *Carbon N. Y.* 47, 1220–1230. doi:10.1016/j.carbon.2008.12.040

Nomura, K., Nishihara, H., Kobayashi, N., Asada, T., and Kyotani, T. (2019a). 4.4 V supercapacitors based on super-stable mesoporous carbon sheet made of edge-free graphene walls. *Energy Environ. Sci.* 12, 1542–1549. doi:10.1039/C8EE03184C

Nomura, K., Nishihara, H., Yamamoto, M., Gabe, A., Ito, M., Uchimura, M., et al. (2019b). Force-driven reversible liquid–gas phase transition mediated by elastic nanosponges. *Nat. Commun.* 10, 2559. doi:10.1038/s41467-019-10511-7

Ohma, A., Furuya, Y., Mashio, T., Ito, M., Nomura, K., Nagao, T., et al. (2021). Elucidation of oxygen reduction reaction and nanostructure of platinum-loaded graphene mesosponge for polymer electrolyte fuel cell electrocatalyst. *Electrochim. Acta* 370, 137705. doi:10.1016/j.electacta.2020.137705

Pantea, D., Darmstadt, H., Kaliaguine, S., and Roy, C. (2003). Heat-treatment of carbon blacks obtained by pyrolysis of used tires. Effect on the surface chemistry, porosity and electrical conductivity. *J. Anal. Appl. Pyrolysis* 67, 55–76. doi:10.1016/S0165-2370(02)00017-7

Park, J., Jung, M., Jang, H., Lee, K., Attia, N. F., and Oh, H. (2018). A facile synthesis tool of nanoporous carbon for promising H2, CO2, and CH4 sorption capacity and selective gas separation. *J. Mater Chem. A Mater* 6, 23087–23100. doi:10.1039/C8TA08603F

Peng, H.-J., Liang, J., Zhu, L., Huang, J.-Q., Cheng, X.-B., Guo, X., et al. (2014). Catalytic self-limited assembly at hard templates: a mesoscale approach to graphene nanoshells for lithium–sulfur batteries. *ACS Nano* 8, 11280–11289. doi:10.1021/nn503985s

Pirabul, K., Pan, Z.-Z., Tang, R., Sunahiro, S., Liu, H., Kanamaru, K., et al. (2023). Structural engineering of nanocarbons comprising graphene frameworks via high-temperature annealing. *Bull. Chem. Soc. Jpn.* 96, 510–518. doi:10.1246/bcsj.20230053

Reina, A., Jia, X., Ho, J., Nezich, D., Son, H., Bulovic, V., et al. (2009). Large area, few-layer graphene films on arbitrary substrates by chemical vapor deposition. *Nano Lett.* 9, 30–35. doi:10.1021/nl801827v

Rodríguez-Mata, V., Gonzalez-Dominguez, J. M., Benito, A. M., Maser, W. K., and García-Bordejé, E. (2019). Reduced graphene oxide aerogels with controlled continuous microchannels for environmental remediation. *ACS Appl. Nano Mater* 2, 1210–1222. doi:10.1021/acsanm.8b02101

Shen, Z., Yu, W., Aziz, A., Chida, K., Yoshii, T., and Nishihara, H. (2023). Sequential catalysis of defected-carbon and solid catalyst in Li–O2 batteries. *J. Phys. Chem. C* 127, 6239–6247. doi:10.1021/acs.jpcc.3c01042

Shi, J.-L., Tang, C., Peng, H.-J., Zhu, L., Cheng, X.-B., Huang, J.-Q., et al. (2015). 3D mesoporous graphene: CVD self-assembly on porous oxide templates and applications in high-stable Li-S batteries. *Small* 11, 5243–5252. doi:10.1002/smll.201501467

Shu, H., Tao, X.-M., and Ding, F. (2015). What are the active carbon species during graphene chemical vapor deposition growth? *Nanoscale* 7, 1627–1634. doi:10.1039/C4NR05590J

Siqueira, J. R., and Oliveira, O. N. (2017). Carbon-based nanomaterials. *Nanostructures*, 233–249. doi:10.1016/B978-0-323-49782-4.00009-7

Su, C.-Y., Lu, A.-Y., Wu, C.-Y., Li, Y.-T., Liu, K.-K., Zhang, W., et al. (2011). Direct Formation of wafer scale graphene thin layers on insulating substrates by chemical vapor deposition. *Nano Lett.* 11, 3612–3616. doi:10.1021/nl201362n

Sun, Z., Fang, S., and Hu, Y. H. (2020). 3D graphene materials: from understanding to design and synthesis control. *Chem. Rev.* 120, 10336–10453. doi:10.1021/acs.chemrev.0c00083

Sunahiro, S., Nomura, K., Goto, S., Kanamaru, K., Tang, R., Yamamoto, M., et al. (2021). Synthesis of graphene mesosponge via catalytic methane decomposition on magnesium oxide. *J. Mat. Chem. A* 9, 14296–14308. doi:10.1039/D1TA02326H

Tang, C., Wang, H.-F., Huang, J.-Q., Qian, W., Wei, F., Qiao, S.-Z., et al. (2019a). 3D hierarchical porous graphene-based energy materials: synthesis, functionalization, and application in energy storage and conversion. *Electrochem. Energy Rev.* 2, 332–371. doi:10.1007/s41918-019-00033-7

Tang, R., Taguchi, K., Nishihara, H., Ishii, T., Morallón, E., Cazorla-Amorós, D., et al. (2019b). Insight into the origin of carbon corrosion in positive electrodes of supercapacitors. *J. Mat. Chem. A* 7, 7480–7488. doi:10.1039/C8TA11005K

Tsakonas, C., Manikas, A. C., Andersen, M., Dimitropoulos, M., Reuter, K., and Galiotis, C. (2021). *In situ* kinetic studies of CVD graphene growth by reflection spectroscopy. *Chem. Eng. J.* 421, 129434. doi:10.1016/j.cej.2021.129434

Vix-Guterl, C., Boulard, S., Parmentier, J., Werckmann, J., and Patarin, J. (2002). Formation of ordered mesoporous carbon material from a silica template by a one-step chemical vapour infiltration process. *Chem. Lett.* 31, 1062–1063. doi:10.1246/cl.2002.1062

Vlassiouk, I., Regmi, M., Fulvio, P., Dai, S., Datskos, P., Eres, G., et al. (2011). Role of hydrogen in chemical vapor deposition growth of large single-crystal graphene. *ACS Nano* 5, 6069–6076. doi:10.1021/nn201978y

Wang, L., Lai, R., Zhang, L., Zeng, M., and Fu, L. (2022). *In situ* investigating the mechanism of graphene growth by chemical vapor deposition. *ACS Mat. Lett.* 4, 528–540. doi:10.1021/acsmaterialslett.1c00783

Xia, T., Yoshii, T., Nomura, K., Wakabayashi, K., Pan, Z.-Z., Ishii, T., et al. (2023). Chemistry of zipping reactions in mesoporous carbon consisting of minimally stacked graphene layers. *Chem. Sci.* 14, 8448–8457. doi:10.1039/D3SC02163G

Yang, G., Li, L., Lee, W. B., and Ng, M. C. (2018). Structure of graphene and its disorders: a review. *Sci. Technol. Adv.* 19, 613–648. doi:10.1080/14686996.2018.1494493

Yoshii, T., Umemoto, D., Yamamoto, M., Kuwahara, Y., Nishihara, H., Mori, K., et al. (2020). Pyrene-Thiol-modified Pd nanoparticles on carbon support: kinetic control by steric hinderance and improved stability by the catalyst-support interaction. *ChemCatChem* 12, 5880–5887. doi:10.1002/cctc.202000987

Yu, W., Shen, Z., Yoshii, T., Iwamura, S., Ono, M., Matsuda, S., et al. (2023a). Hierarchically porous and minimally stacked graphene cathodes for high-performance lithium–oxygen batteries. *Adv. Energy Mater n/a*, 2303055. doi:10.1002/aenm.202303055

Yu, W., Yoshii, T., Aziz, A., Tang, R., Pan, Z.-Z., Inoue, K., et al. (2023b). Edge-site-free and topological-defect-rich carbon cathode for high-performance lithium-oxygen batteries. *Adv. Sci.* 10, 2300268. doi:10.1002/advs.202300268

Zhang, F., Zhu, D., Chen, X., Xu, X., Yang, Z., Zou, C., et al. (2014). A nickel hydroxide-coated 3D porous graphene hollow sphere framework as a high performance electrode material for supercapacitors. *Phys. Chem. Chem. Phys.* 16, 4186–4192. doi:10.1039/C3CP54334J

Zhang, L., Alvarez, N. T., Zhang, M., Haase, M., Malik, R., Mast, D., et al. (2015). Preparation and characterization of graphene paper for electromagnetic interference shielding. *Carbon N. Y.* 82, 353–359. doi:10.1016/j.carbon.2014.10.080